

Energy levels distribution in supersaturated silicon with titanium for photovoltaic applications

E. Pérez, H. Castán, H. García, S. Dueñas, L. Bailón, D. Montero, R. García-Hernansanz, E. García-Hemme, J. Olea, and G. González-Díaz

Citation: *Applied Physics Letters* **106**, 022105 (2015); doi: 10.1063/1.4905784

View online: <http://dx.doi.org/10.1063/1.4905784>

View Table of Contents: <http://scitation.aip.org/content/aip/journal/apl/106/2?ver=pdfcov>

Published by the [AIP Publishing](#)

Articles you may be interested in

[Electrical levels in nickel doped silicon](#)

J. Appl. Phys. **116**, 173704 (2014); 10.1063/1.4901003

[Electron and hole deep levels related to Sb-mediated Ge quantum dots embedded in n-type Si, studied by deep level transient spectroscopy](#)

Appl. Phys. Lett. **102**, 232106 (2013); 10.1063/1.4809595

[Copper centers in copper-diffused n-type silicon measured by photoluminescence and deep-level transient spectroscopy](#)

Appl. Phys. Lett. **101**, 042113 (2012); 10.1063/1.4739470

[Characterization of deep-levels in silicon nanowires by low-frequency noise spectroscopy](#)

Appl. Phys. Lett. **99**, 113107 (2011); 10.1063/1.3637049

[Field-enhanced ionization of deep-level centers as a triggering mechanism for superfast impact ionization fronts in Si structures](#)

J. Appl. Phys. **98**, 094506 (2005); 10.1063/1.2125118

The advertisement features a photograph of the Model PS-100 cryogenic probe station, which is a complex piece of scientific equipment with various mechanical components and a probe. The background is a gradient of blue. The text is arranged around the image: the model name and description on the left, the company logo and name in the center, and a slogan on the right.

Model PS-100
Tabletop Cryogenic
Probe Station



Lake Shore
CRYOTRONICS

*An affordable solution for
a wide range of research*

Energy levels distribution in supersaturated silicon with titanium for photovoltaic applications

E. Pérez,^{1,a)} H. Castán,¹ H. García,¹ S. Dueñas,¹ L. Bailón,¹ D. Montero,^{2,3}
 R. García-Hernansanz,^{2,3} E. García-Hemme,^{2,3} J. Olea,^{3,4} and G. González-Díaz^{2,3}

¹*Dept. de Electricidad y Electrónica, Universidad de Valladolid, ETSI Telecomunicación, Paseo de Belén 15, 47011 Valladolid, Spain*

²*Dept. de Física Aplicada III (Electricidad y Electrónica), Univ. Complutense de Madrid, 28040 Madrid, Spain*

³*CEI Campus Moncloa, UCM-UPM, 28040 Madrid, Spain*

⁴*Instituto de Energía Solar, E.T.S.I. de Telecomunicación, Univ. Politécnica de Madrid, 28040 Madrid, Spain*

(Received 14 November 2014; accepted 30 December 2014; published online 12 January 2015)

In the attempt to form an intermediate band in the bandgap of silicon substrates to give it the capability to absorb infrared radiation, we studied the deep levels in supersaturated silicon with titanium. The technique used to characterize the energy levels was the thermal admittance spectroscopy. Our experimental results showed that in samples with titanium concentration just under Mott limit there was a relationship among the activation energy value and the capture cross section value. This relationship obeys to the well known Meyer-Neldel rule, which typically appears in processes involving multiple excitations, like carrier capture/emission in deep levels, and it is generally observed in disordered systems. The obtained characteristic Meyer-Neldel parameters were $T_{mn} = 176$ K and $kT_{mn} = 15$ meV. The energy value could be associated to the typical energy of the phonons in the substrate. The almost perfect adjust of all experimental data to the same straight line provides further evidence of the validity of the Meyer Neldel rule, and may contribute to obtain a deeper insight on the ultimate meaning of this phenomenon. © 2015 AIP Publishing LLC. [<http://dx.doi.org/10.1063/1.4905784>]

The study of silicon substrates supersaturated with Ti is of great interest nowadays. The main goal of these studies is the formation of an intermediate band (IB) in the midgap of the semiconductor to induce infrared absorption in this material.^{1,2} This approach would enable electrons to be pumped from the valence band (VB) into conduction band (CB) via two-photon absorption with lower energy than the semiconductor band gap.³ There are two main reasons why obtaining this target is so interesting. The first one is to improve the efficiency of solar cells based on silicon. Single junction silicon solar cells with IB could reach efficiency values up to 63.1%,⁴ above the maximum theoretical efficiency for single junction cells established by Shockley and Queisser in 40.7%.^{4,5} The second reason is that silicon-based devices capable to absorb infrared radiation can reduce the cost and fabrication complexity of infrared detectors.⁶ To obtain this IB is necessary that the Ti concentration exceed the Mott limit ($5.9 \times 10^{19} \text{ cm}^{-3}$).^{3,7}

In order to carry out our study, $300 \mu\text{m}$ Si (111) n-type samples ($\mu = 1450 \text{ cm}^2/\text{V s}$; $n = 2.2 \times 10^{13} \text{ cm}^{-3}$ at room temperature) were implanted in an ion beam service (IBS) refurbished VARIAN CF3000 Ion Implanter at 32 keV with Ti at high doses: 10^{13} (UM1), 10^{14} (UM2), 10^{15} (OM1), and 10^{16} (OM2) cm^{-2} . Bottom and top electrodes were fabricated by aluminum evaporation. To obtain good ohmic contacts on the bottom, n^+ layers were fabricated on the back side of the samples by ion implantation of phosphorous in a dose of 10^{15} cm^{-2} at energy of 80 keV. Afterwards, samples were annealed at 900°C during 20 s. Schottky contacts were

fabricated in the top by aluminum evaporation. Then, the implanted Si samples were annealed by means of the pulsed laser melting (PLM) method to recover the crystal lattice.⁸ The PLM annealing process was performed by IPG Photonics (New Hampshire, USA). Samples were annealed with one 20 ns long pulse of a KrF excimer laser (248 nm) at energy density of 0.8 J/cm^2 . UM1 and UM2 samples have Ti implantation profiles below the Mott limit at any depth. OM1 and OM2 samples have Ti profiles over the Mott limit up to 20 and 80 nm, respectively.⁹

Samples were studied by means of Thermal Admittance Spectroscopy (TAS) technique,¹⁰ which yields thermal emission rates of deep levels from the variations of capacitance and conductance of a p-n or Schottky junction as a function of temperature and frequency. These variations are due to the change in frequency of the measuring signal with respect to the time constants of charge and discharge processes of the deep levels. Measurements consist on recording the capacitance and conductance variation of a bipolar junction as a function of temperature at a given frequency. Each deep level existing in the semiconductor band gap contributes with a peak in the conductance signal, which is related to the deep level emission rate by the well-known equation

$$e^{\omega(T_{peak})} = \omega/1.98, \quad (1)$$

where ω is the angular frequency. The activation energy and the capture cross section of the deep level can be obtained from the Arrhenius plot of experimental data¹¹

$$e^{\omega(T)} = \sigma_T v_{th} N_C \times \exp(-E_T/kT). \quad (2)$$

^{a)}Electronic mail: eduper@ele.uva.es

TABLE I. Experimental results of the analyzed samples. The voltage bias values applied (Bias), as well as the obtained activation energy (E_T) and capture cross section (σ_T) values, are listed.

Sample	Bias (V)	E_T (meV)	σ_T (cm ²)
UM1	-7.5	454	8.71×10^{-8}
	-5	307	5.50×10^{-12}
	-4	290	2.94×10^{-12}
	-3	233	1.09×10^{-13}
		451	2.23×10^{-7}
	-2	173	2.39×10^{-15}
		460	4.08×10^{-7}
	-1	88	3.85×10^{-18}
		427	1.65×10^{-8}
		0	391
UM2	-7.5	365	2.88×10^{-10}
	-5	335	6.91×10^{-11}
	-4	303	8.46×10^{-12}
	-3	238	1.11×10^{-13}
	-2	193	8.13×10^{-15}
	-1.25	129	1.19×10^{-16}
		277	3.20×10^{-12}
	-1	86	3.92×10^{-18}
		264	7.70×10^{-13}
	-0.75	66	1.44×10^{-18}
	274	2.40×10^{-12}	
	0	287	3.07×10^{-12}

Table I shows the activation energy (E_T) and capture cross section (σ_T) values obtained at different bias values in samples with Ti concentrations just under the Mott limit. In the samples with Ti concentrations over the Mott limit is not possible to apply the TAS technique. As we show in Fig. 1, this kind of samples have an ohmic behavior instead of the rectifier behavior that we need to be able to apply TAS. Fig. 1 also shows that UM1 and UM2 fulfill this requirement. Only room-temperature I-V curves are shown in this figure, but similar results were obtained for the entire experimental temperature range (77–300 K).

These results are also supported by C-V curves (at room temperature) of Fig. 2. In the case of OM1 and OM2, the Fermi level is locked near to the defect band. This fact makes that there is no depletion region modulation as Fig. 2 shows, being C-V curves from these samples almost constant

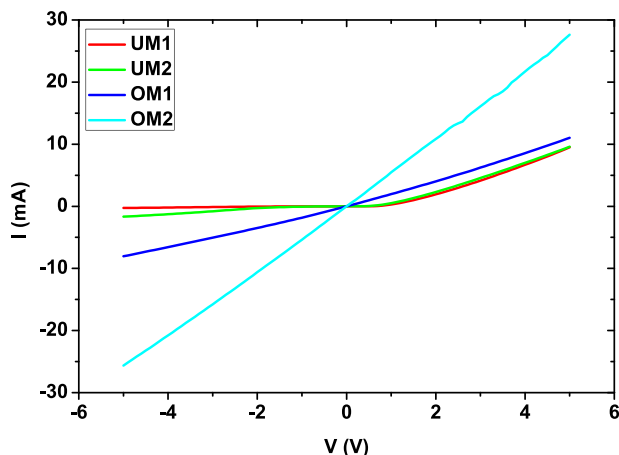


FIG. 1. I-V curves for all samples at room temperature.

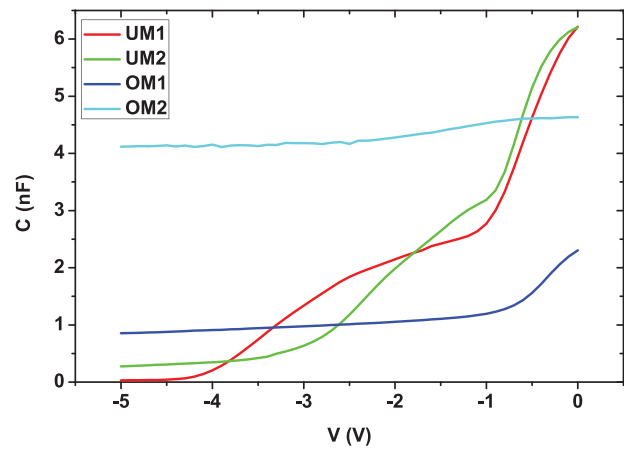


FIG. 2. C-V curves for all samples at room temperature.

with bias change. Therefore, it is not possible to use the TAS technique over them. In contrast, UM1 and UM2 samples exhibit strong dependence of their capacitance with the bias voltage, so indicating that a depletion layer modulation occurs. That is the reason why TAS technique allows us to characterize deep levels on samples with Ti concentration under Mott limit.

Table I shows that depending on the bias voltage value, one or two energy levels were obtained. Varying the bias voltage means changing the depletion region depth, thus the specific physical region under study. For example, in UM1 sample biased at 0 V a single deep level was detected. Fig. 3 shows that each conductance curve has only one peak. The activation energy of this level was obtained from the corresponding Arrhenius plot (Fig. 4). In contrast, for -1, -2, and -3 V bias values, two different deep levels were detected. For bias values of -4, -5 V, and beyond, only one deep was detected again. A similar behavior is observed in UM2 sample. As an example, we can see in Fig. 5 the existence of two deep levels at -1 V. The associated Arrhenius plot of these two levels are shown in Fig. 6.

A thorough examination of Table I reveals that there is a clear dependency among capture cross section and activation energy for all deep levels detected. Fig. 7 shows that this dependence fits to a linear relationship that follows the Meyer-Neldel (MN) rule.^{12,13} As it is known, this rule establishes

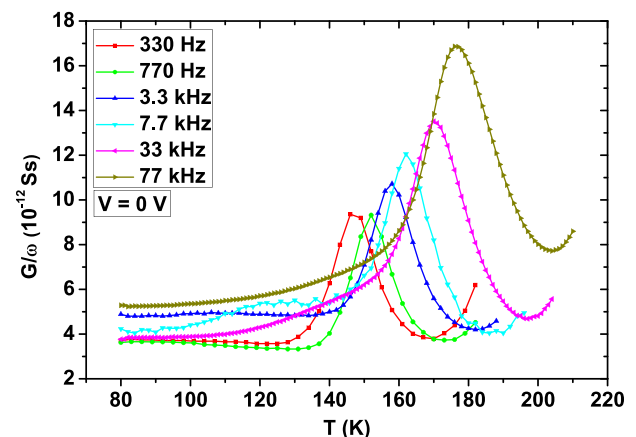


FIG. 3. G/ω -T curves for the UM1 sample biased at 0 V.

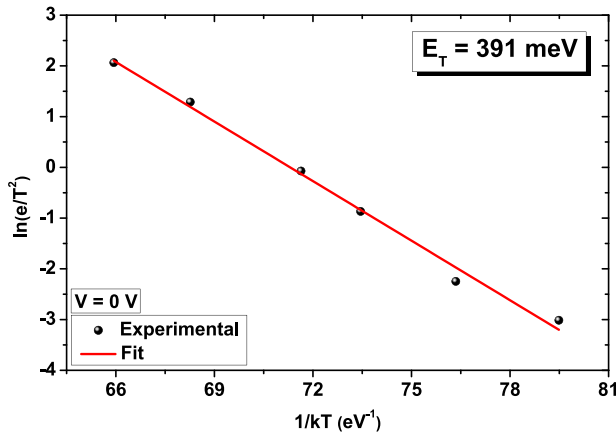


FIG. 4. Arrhenius plot for the UM1 sample biased at 0 V.

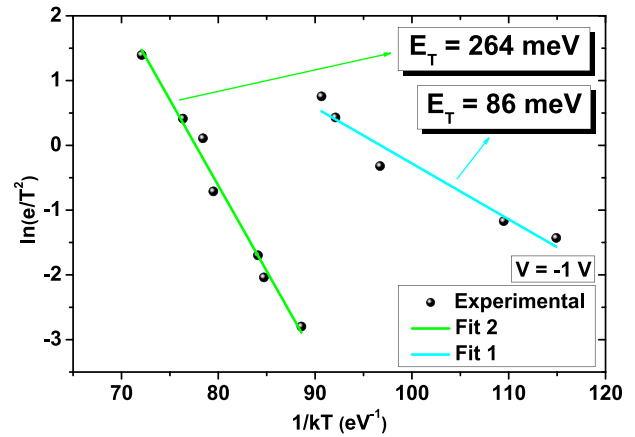


FIG. 6. Arrhenius plot for the UM2 sample biased at -1 V.

that there is a relation between the pre-exponential factor and the activation energy as follows:

$$\sigma_T = \sigma_{TT} \times \exp(E_T/kT_{mn}) \quad (3)$$

in magnitudes with an Arrhenius dependence, as the emission rate of a deep level (Eq. (2)). T_{mn} is called MN temperature and kT_{mn} the MN energy, assuming that v_{th} and N_C remains constant with the variation of the activation energy. Fig. 7 shows that all experimental values corresponding to both samples fit very well to the same straight line, whose slope provides a value of 15 meV for kT_{mn} ($T_{mn} = 176$ K).

MN rule behavior has been found in various different systems. Frequently MN rule is reported for electrical properties such as the conductivity or for diffusion measurements. There are quite a few references reporting this behavior in different magnitudes in semiconductor devices, such as the trap distribution in semiconductor samples.¹³ Widenhorn *et al.* calculated the MN rule for the dark current in a silicon CCD and found an energy value of 25.3 meV.¹⁴ The same authors reported an energy value of 56.5 meV for forward current in diodes.¹⁵ Coutts and Pearsall found 31 meV for the reverse current of solar cells.¹⁶ Other works report values of energy under 10 meV: Antonov *et al.* found a MN energy of 6.9 meV in the diffusion of nanoclusters and

islands on solid Xe.¹⁷ The same group¹⁸ studied nanoclusters and islands on CO₂, obtaining a MN energy of approximately 9 meV, in agreement with the most active phonon band for solid CO₂.

It has been pointed out that because of the variety of situations where this rule appears, it is very likely that the explanation is not associated to a particular process, but to a more fundamental phenomenon, such as Multi Excitation Entropy (MEE) theory.¹⁹ It would be required the accumulation or annihilation of a large number of excitations for a kinetic event to take place. In spite of that the MN rule is generally observed in disordered systems where processes involve multiple excitations,²⁰ for instance, carrier capture or emission in deep levels,²¹ in a recent paper Yelon²² claimed that it is extremely unlikely that T_{mn} values represent a measure of disorder, increasing with it. Instead, virtually all solid-state phenomena give values of kT_{mn} that can be associated to the typical phonon energies.

In conclusion, our study of the deep levels energy distribution on the disordered silicon substrates supersaturated with Ti clearly demonstrates that the relationship between the activation energy and capture cross section values of all deep levels detected by means of TAS technique in the two samples analyzed obeys to the MN rule. The values obtained from the linear fit for the characteristic temperature and

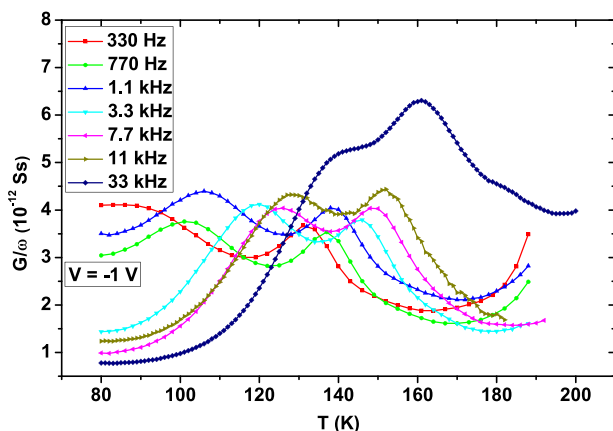


FIG. 5. G/ω - T curves for the UM2 sample biased at -1 V.

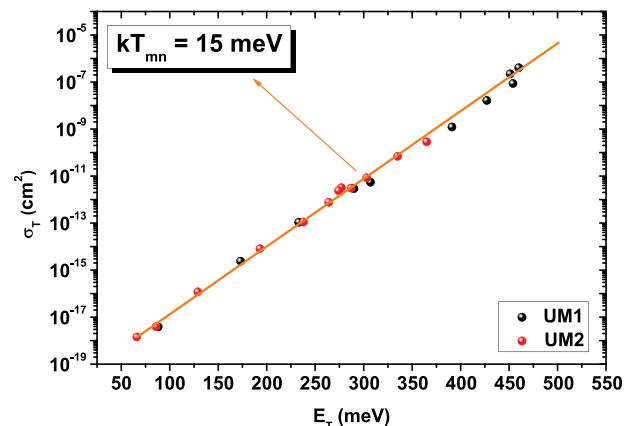


FIG. 7. Capture cross section vs. activation energy for all bias values in both UM1 and UM2 samples.

energy of this phenomenon are, respectively, $T_{mn} = 176$ K and $kT_{mn} = 15$ meV. This last value could be related to the energy of the phonons involved in the carrier emission/capture process in Ti deep levels.

The study has been supported by the Spanish TEC2011 under Grant No. 27292-C02-01, TEC2013-41730-R funded by the Ministerio de Economía y Competitividad, and the P2013/MAE-2780 funded by the Comunidad de Madrid. Research of E. Pérez was supported by a University of Valladolid FPI Grant. J. Olea acknowledge financial support from the MICINN within the program Juan de la Cierva (JCI-2011-10402), under which this research was undertaken. Research by E. García-Hemme was also supported by a PICATA predoctoral fellowship of the Moncloa Campus of International Excellence (UCM-UPM).

¹J. Olea, D. Pastor, M. T. Luque, I. Mártil, and G. González, *Next Generation of Photovoltaics. New Concepts*, Springer Series in Optical Sciences (Springer, 2012), pp. 321–346.

²H. Castán, E. Pérez, H. García, S. Dueñas, L. Bailón, J. Olea, D. Pastor, E. García-Hemme, M. Irigoyen, and G. González-Díaz, *J. Appl. Phys.* **113**, 024104 (2013).

³G. González-Díaz, J. Olea, I. Mártil, D. Pastor, A. Martí, E. Antolín, and A. Luque, *Sol. Energy Mater. Sol. Cells* **93**, 1668 (2009).

⁴A. Luque and A. Martí, *Phys. Rev. Lett.* **78**, 5014 (1997).

⁵A. Luque and A. Martí, *Handbook of Photovoltaic Science and Engineering*, 2nd ed. (John Wiley & Sons, 2011), pp. 130–168.

⁶J. Mailoa, A. Akey, C. Simmons, D. Hutchinson, J. Mathews, J. T. Sullivan, D. Recht, M. Winkler, J. Williams, J. Warrender, P. Persans, M. Aziz, and T. Buonassisi, *Nat. Commun.* **5**, 3011 (2014).

⁷A. Luque, A. Martí, E. Antolín, and C. Tablero, *Phys. B* **382**, 320 (2006).

⁸J. Olea, M. Toledano-Luque, D. Pastor, E. San-Andrés, I. Mártil, and G. González-Díaz, *J. Appl. Phys.* **107**, 103524 (2010).

⁹J. Olea, D. Pastor, M. Toledano-Luque, I. Mártil, and G. González-Díaz, *J. Appl. Phys.* **110**, 064501 (2011).

¹⁰J. Barbolla, S. Dueñas, and L. Bailón, *Solid-State Electron.* **35**, 285 (1992).

¹¹D. K. Schroder, *Semiconductor Material and Device Characterization*, 2nd ed. (John Wiley & Sons, 1998).

¹²W. Meyer and H. Neldel, *Z. Tech. Phys.* **18**, 588 (1937).

¹³Y. Chen and S. Huang, *Phys. Rev. B* **44**, 13775 (1991).

¹⁴R. Widenhorn, L. Mundermann, A. Rest, and E. Bodegom, *J. Appl. Phys.* **89**, 8179 (2001).

¹⁵R. Widenhorn, M. Fitzgibbons, and E. Bodegom, *J. Appl. Phys.* **96**, 7379 (2004).

¹⁶T. Coutts and N. Pearsall, *Appl. Phys. Lett.* **44**, 134 (1984).

¹⁷V. Antonov, J. Palmer, P. Waggoner, A. Bhatti, and J. Weaver, *Phys. Rev. B* **70**, 045406 (2004).

¹⁸P. Waggoner, J. Palmer, V. Antonov, and J. Weaver, *Surf. Sci.* **596**, 12 (2005).

¹⁹A. Yelon, B. Movaghar, and R. Crandall, *Rep. Prog. Phys.* **69**, 1145 (2006).

²⁰A. Yelon, B. Movaghar, and H. Branz, *Phys. Rev. B* **46**, 12244 (1992).

²¹D. Lang and C. Henry, *Phys. Rev. Lett.* **35**, 1525 (1975).

²²A. Yelon, *Monatsh. Chem.* **144**, 91 (2013).